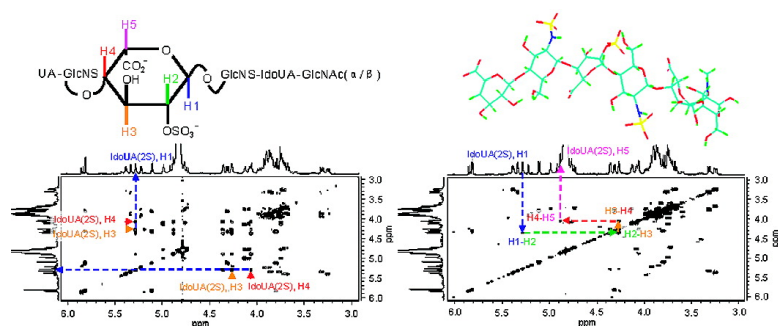Article

Structural Studies of Heparan Sulfate Hexasaccharides: New Insights into Iduronate Conformational Behavior

Kevin J. Murphy, Neil McLay, and David A. Pye

More About This Article

Additional resources and features associated with this article are available within the HTML version:

- Supporting Information
- Access to high resolution figures
- Links to articles and content related to this article
- Copyright permission to reproduce figures and/or text from this article

View the Full Text HTML

Structural Studies of Heparan Sulfate Hexasaccharides: New Insights into Iduronate Conformational Behavior

Kevin J. Murphy,[†] Neil McLay,[†] and David A. Pye[*,†,‡]

*Department of Chemical and Biological Sciences, University of Huddersfield, Huddersfield
HD1 3DH, United Kingdom, and Centre for Molecular Drug Design, Cockcroft Building,
University of Salford, Manchester M5 4WT, United Kingdom*

Received April 18, 2008; E-mail: d.pye@salford.ac.uk

Abstract: There is a growing opinion that the conformational dynamics within HS chains is critical to their observed biological activities. Investigations into HS conformational dynamics are problematic, given the structural complexity and heterogeneity of HS chains. However, this goal will be more obtainable once we understand the important roles HS sequence/sulfation patterns play in determining the conformational dynamics of iduronate units. This is the first study to compare isomers of *N*-sulfated oligosaccharides, with respect to the conformational versatility of their internal iduronates. Characterization by NMR spectroscopy of two HS oligosaccharides derived from porcine mucosal HS enabled the measurement of iduronate coupling constants, while under the influence of different flanking saccharide sequences. By fitting our coupling constant data to a new set of theoretical coupling constants, calculated using explicit water molecular dynamic simulations, we are able to offer new insights into the role sequence/sulfation patterns play in influencing iduronate conformational behavior. Fitting of experimental data, using our new theoretically derived coupling constants, suggests that replacement of the *N*-sulfate group to the reducing side of IdoUA by an *N*-acetyl group has little effect on the balance of IdoUA conformational equilibrium. Fitting of coupling constants for sequences GlcNS-IdoUA(2S)-GlcNS and GlcNS(6S)-IdoUA(2S)-GlcNS suggests that the flanking 6-*O*-sulfate group alters the balance of the IdoUA(2S) equilibrium more toward the $^2S_0$ conformation. There is also the suggestion that a cooperative effect may exist for *N*- and 6-*O* sulfation. These observations could be the key to understanding the important regulatory function attributed to 6-*O*-sulfation within HS chains.

Introduction

Heparan sulfate (HS) is a glycosaminoglycan (GAG) made up of a repeating 1,4- linked disaccharide unit. This is composed of a hexuronic acid, one of either glucuronic acid (GlcUA) or iduronic acid (IdoUA) and an *N*-acetyl (GlcNAc) or *N*-sulfo-glucosamine (GlcNS). In addition to *N*-sulfation, many of these constituent disaccharides bear one or several *O*-sulfo substituents. Commonly *O*-sulfation occurs at C-2 of IdoUA to form the monosaccharide 2-*O*-sulfo iduronic acid (IdoUA(2S)) and/ or at C-6 of GlcNS or GlcNAc to form the monosaccharides 6-*O*-*N*-sulfo-glucosamine (GlcNS(6S)) and 6-*O*-sulfo-*N*-acetyl-glucosamine (GlcNAc(6S)). Sulfated disaccharides mainly occur in blocks termed "S-domains"; these are separated by stretches of the none sulfated disaccharide GlcUA(1−4)GlcNAc, which is predominant, and typically makes up around 50% of the total disaccharide units.[1,2]

It is well recognized that various short-chain HS oligosaccharides have the ability to interact with protein ligands and regulate their biological activity. To date, these oligosaccharides have been solely made up of or contain clusters of sulfated residues. In some notable cases, for example, antithrombin III,[3] fibroblast growth factor-1 (FGF-1),[4−7] and fibroblast growth factor-2 (FGF-2),[8−10] the interactions/biological activity of HS oligosaccharides has been shown to be dependent on a critical sequence of sulfated monosaccharides. In others cases, for example, hepatocyte growth factor/scatter factor[11] and vascular endothelial growth factor,[12] a predominance of a particular sulfation position, in these cases 6-*O*-sulfation over 2-*O*-sulfation or *N*-sulfation, has been shown to be important.

† University of Huddersfield.

‡ University of Salford.

(1) Maccarana, M.; Sakura, Y.; Tawada, A.; Yoshida, K.; Lindahl, U. *J. Biol. Chem.* **1996**, *271*, 17804–10.

(2) Murphy, K. J.; Merry, C. L. R.; Lyon, M.; Thompson, J. E.; Roberts, I. S.; Gallagher, J. T. *J. Biol. Chem.* **2004**, *279*, 27239–27245.

(3) Jin, L.; Abrahams, J. P.; Skinner, R.; Petitou, M.; Pike, R. N.; Carrell, R. W. *Proc. Natl. Acad. Sci. U.S.A.* **1997**, *94*, 14683–8.

(4) Jemth, P.; Kreuger, J.; Kusche-Gullberg, M.; Sturiale, L.; Gimenez-Gallego, G.; Lindahl, U. *J. Biol. Chem.* **2002**, *277*, 30567–73.

(5) Kreuger, J.; Jemth, P.; Sanders-Lindberg, E.; Eliahu, L.; Ron, D.; Basilico, C.; Salmivirta, K.; Lindahl, U. *Biochem. J.* **2005**, *389*, 145–150.

(6) Kreuger, J.; Salmivirta, M.; Sturiale, L.; Gimenez-Gallego, G.; Lindahl, U. *J. Biol. Chem.* **2001**, *276*, 30744–52.

(7) Pye, D. A.; Vives, R. R.; Hyde, P.; Gallagher, J. T. *Glycobiology* **2000**, *10*, 1183–92.

(8) Maccarana, M.; Casu, B.; Lindahl, U. *J. Biol. Chem.* **1993**, *268*, 23898–905.

(9) Turnbull, J. E.; Fernig, D. G.; Ke, Y.; Wilkinson, M. C.; Gallagher, J. T. *J. Biol. Chem.* **1992**, *267*, 10337–41.

(10) Pye, D. A.; Vives, R. R.; Turnbull, J. E.; Hyde, P.; Gallagher, J. T. *J. Biol. Chem.* **1998**, *273*, 22936–42.

(11) Lyon, M.; Deakin, J. A.; Mizuno, K.; Nakamura, T.; Gallagher, J. T. *J. Biol. Chem.* **1994**, *269*, 11216–23.

(12) Ono, K.; Hattori, H.; Takeshita, S.; Kurita, A.; Ishihara, M. *Glycobiology* **1999**, *9*, 705–11.
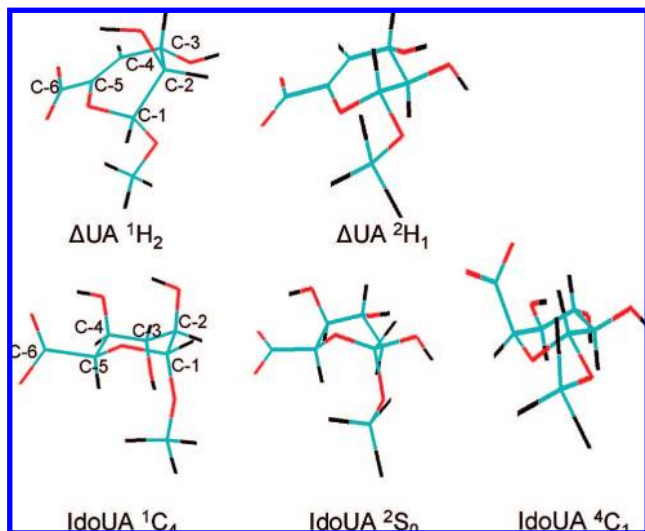
Figure 1. The low-energy conformations of the conformationally variable monosaccharides Δ4,5 uronic acid (ΔUA) and α-L-iduronic acid (IdoUA). These residues may also occur as sulfated derivatives with an *O*-sulfo group attached to carbon position 2 (C-2) (see Introduction).

S-domain oligosaccharides of varying length and sulfation pattern can be excised from polymeric HS through the action of the enzyme heparinase III.[13,14] Oligosaccharides generated in this way contain unsaturated uronic acid residues (ΔUA) at their nonreducing end. However, due to the extreme difficulty in obtaining large quantities of homogeneous sample, many researchers have instead used synthetic or heparin-derived oligosaccharides as models for S-domain structures.

It is well established that the conformation of the hexopyranose residues of most common carbohydrates is in one of two low energy chair forms, $^4C_1$ or $^1C_4$. IdoUA and IdoUA(2S) (collectively termed iduronates)[15] vary in conformation between the two above-mentioned chair forms and an additional $^2S_0$ skew boat conformation (Figure 1), with the equilibrium influenced by the sulfation state of neighboring glucosamine residues. This confers additional conformational flexibility within the S-domains and may be of importance in specific protein binding and recognition events. This is highlighted by the X-ray crystal structure of a hexasaccharide/FGF-2 complex.[16] In this structure, the two internal IdoUA(2S) residues are present in alternate conformations, $^1C_4$ and $^2S_0$; this has the effect of increasing the oligosaccharides area of contact with the protein surface. When positioned internally within an oligosaccharide, the $^1C_4$ and $^2S_0$ conformations are thought to predominate.[17] The important role sulfation patterns may play in influencing this conformational equilibrium has been alluded to in studies on the antithrombin III (ATIII) binding pentasaccharide. Rather than interacting directly with the ATIII, the role of a number of sulfate groups may be to influence the conformational equilibrium of a neighboring IdoUA toward the $^2S_0$ conformation.[18] Only those oligosaccharides containing IdoUA in the $^2S_0$

conformation had the ability to bind and activate ATIII in a factor Xa inhibition assay.[19] However, it has been shown recently that the contribution of IdoUA(2S) to antithrombin binding affinity is less essential once the size of an oligosaccharide is longer than an octasaccharide.[20] The same study also showed that long-chain length oligosaccharide mixtures do not need any iduronates to possess anticoagulant activity. Yet it should be noted that the authors still showed IdoUA(2S) to be a requirement for FGF2 activation of the FGFR1c receptor.

The ΔUA terminal residue also varies in conformation, between two half-chair forms, $^2H_1$ and $^1H_2$ (Figure 1).[21] Like iduronate, the position of this conformational equilibrium may also influence the oligosaccharides biological activity. This will not be relevant for intact HS chains; however, the X-ray crystal structure of a dimeric 2:2:2 decasaccharide/FGFR1/FGF-2 crystal complex shows a number of interactions between each of the two ΔUA terminal residues and one or the other of the two FGFR1 monomers.[22]

Although HS itself has been available in bulk quantities for a number of years,[23] very few authentic HS-derived oligosaccharides, larger than dp4, have been characterized by conformational analysis based on NMR spectral parameters.[24] This is due to the extreme difficulty in obtaining homogeneous samples in the quantities required for NMR analysis. The number of potential sulfation sequences, and consequently sample heterogeneity, increases dramatically with chain length, as seen in HPLC profiles and electrophoretic separations.[25] This is another important factor given the typical correlations seen between increasing chain length and binding affinity/biological activity. The monosaccharide sequence of a number of radio-labeled HS oligosaccharides has been established;[6,26,27] however, the small quantities available precluded their use in NMR studies.

Here, we describe the NMR spectroscopy study and conformational analysis of two previously uncharacterized HS hexasaccharides, obtained from porcine intestinal mucosal HS. Analysis of coupling constant data has allowed the determination of the predominant conformation for all iduronate and ΔUA residues present. Comparisons with several similarly conformationally characterized synthetic and naturally derived structures, provide additional insight into the influence of sulfation pattern on conformational equilibria within HS chains. This information may be crucial, given that in all cases to date it

(13) Desai, U. R.; Wang, H. M.; Linhardt, R. J. *Arch. Biochem. Biophys.* **1993**, *306*, 461–8.
(14) Linhardt, R. J.; Turnbull, J. E.; Wang, H. M.; Loganathan, D.; Gallagher, J. T. *Biochemistry* **1990**, *29*, 2611–7.
(15) Mulloy, B.; Forster, M. J. *Glycobiology* **2000**, *10*, 1147–56.
(16) Faham, S.; Hileman, R. E.; Fromm, J. R.; Linhardt, R. J.; Rees, D. C. *Science* **1996**, *271*, 1116–20.
(17) Ferro, D. R.; Provasoli, A.; Ragazzi, M.; Casu, B.; Torri, G.; Bossennec, V.; Perly, B.; Sinay, P. *Carbohydr. Res.* **1990**, *195*, 157–167.

(18) Sisu, E.; Tripathy, S.; Mallet, J. M.; Driguez, P. A.; Herault, J. P.; Sizun, P.; Herbert, J. M.; Petitou, M.; Sinay, P. *Biochimie* **2003**, *85*, 91–99.
(19) Das, S. K.; Mallet, J. M.; Esnault, J.; Driguez, P. A.; Duchaussoy, P.; Sizun, P.; Herault, J. P.; Herbert, J. M.; Petitou, M.; Sinay, P. *Angew. Chem., Int. Ed.* **2001**, *40*, 1670–1673.
(20) Chen, J.; Jones, C. L.; Liu, J. *Chem. Biol.* **2007**, *14*, 986–993.
(21) Raggazzi, M.; Ferro, D. R.; Provasoli, A.; Pumilia, P.; Cassinari, A.; Torri, G.; Guerrini, M.; Casu, B.; Nader, H. B.; Dietrich, C. P. *J. Carbohydr. Chem.* **1993**, *12*, 523–535.
(22) Schlessinger, J.; Plotnikov, A. N.; Ibrahimi, O. A.; Eliseenkova, A. V.; Yeh, B. K.; Yayon, A.; Linhardt, R. J.; Mohammadi, M. *Mol. Cell* **2000**, *6*, 743–750.
(23) Griffin, C. C.; Linhardt, R. J.; Van Gorp, C. L.; Toida, T.; Hileman, R. E.; Schubert, R. L.; Brown, S. E. *Carbohydr. Res.* **1995**, *276*, 183–197.
(24) Hileman, R. E.; Smith, A. E.; Toida, T.; Linhardt, R. J. *Glycobiology* **1997**, *7*, 231–239.
(25) Vives, R. R.; Goodger, S. J.; Pye, D. A. *Biochem. J.* **2001**, *354*, 141–147.
(26) Vives, R. R.; Pye, D. A.; Salmivirta, M.; Hopwood, J. J.; Lindahl, U.; Gallagher, J. T. *Biochem. J.* **1999**, *339*, 767–73.
(27) Merry, C. L.; Lyon, M.; Deakin, J. A.; Hopwood, J. J.; Gallagher, J. T. *J. Biol. Chem.* **1999**, *274*, 18455–62.

has not been possible to link HS sequence/sulfation patterns directly to specific biological activities.

Materials and Methods

Bio-Gel P-10 (fine grade) was purchased from Bio-Rad (Hemel Hempsted, Herts, UK). PD-10 prepacked, disposable Sephadex G-25 columns were purchased from Amersham Pharmacia Biotech. ProPac PA-1 analytical strong anion-exchange HPLC columns were from Dionex (Camberley, Surrey, UK). Heparinase I (*Flavobacterium heparinum*; EC 4.2.2.7), heparinase II (*F. heparinum*; no EC number assigned), and heparinase III (*F. heparinum*; EC 4.2.2.8) were purchased from Grampian Enzymes (Orkney, UK). Porcine intestinal mucosal heparan sulfate was purchased from Celsus laboratories (Cincinnati, OH). D_2O was purchased from GOSS scientific (Essex UK). Acrylamide and HPLC grade sodium chloride were purchased from VWR international (Poole, UK). Trizma-base, Glycine, Azure A, and a Shigemi NMR microtube matched to D_2O were obtained from Sigma-Aldrich (Dorset, UK).

Enzymatic Depolymerization of HS. Porcine intestinal mucosal HS was depolymerized using the enzyme heparinase III. To 200 mg of HS were added 2 mL of 0.1 mM sodium acetate, 0.1 mM calcium acetate, pH 7.0, and 10 mU of heparinase III. Initial studies showed that three subsequent additions of 10 mU of heparinase III at 16 h intervals at 25 °C affected complete digestion (data not shown). In total, 50 identical digests were carried out using 10 g of HS starting material.

Gel Filtration Chromatography. Each 200 mg digest was applied to a Bio-Gel P10 column (3 × 120 cm) eluted with 0.25 M NH_4HCO_3 at a flow rate of 9 mL h^{-1}. Fractions were collected (3 mL), their absorbance at 232 nm was measured, and relevant fractions were pooled and lyophilized. After initial lyopholization, the concentration of NH_4^+ ions was further reduced by repeatedly redissolving the samples in 10 mL of H_2O and evaporating to dryness using rotary evaporation.

Strong Anion-Exchange HPLC (SAX-HPLC). Hexasaccharide samples were applied to a ProPac PA-1 column (9 × 250 mm) pre-equilibrated with distilled water adjusted to pH 3.5 with HCl. Elution was achieved with a NaCl gradient of 0–1 M NaCl over 80 min at a flow rate of 4 mL min^{-1}. The eluate was monitored in-line for absorbance at 232 nm, and fractions (2 mL) were collected. Relevant fractions were pooled and added to identical fractions from previous separation runs. These were concentrated by rotary evaporation, desalted on a PD10 column eluted with water, and then lyophilized.

Polyacryamide Gel Electrophoresis (PAGE). To each well was loaded 10 μg of hexasaccharide in 20 μL of a 20% (v/v) glycerol, 1% (w/v) phenol red solution. Samples were initially run through a 1.5 cm stacking gel (5% acrylamide/2% cross-linker), and then through a 16 cm × 12 cm × 0.75 cm resolving gel (30% acrylamide/5% cross-linker) at a constant voltage of 200 V until the phenol red marker reached the bottom of the gel. The discontinuous buffer system of Laemmli was used[28] with 0.375 M Tris/HCl in the resolving gel and 0.125 M Tris/HCl in the stacking gel at pH's of 8.5 and 6.5, respectively. Tank buffer consisted of 25 mM Tris/0.192 M glycine pH 8.3. Oligosaccharide bands were visualized by staining with 0.25% (w/v) aqueous Azure A for 5 min under constant agitation. Gels were destained by repeated washing in water for up to 30 min.

Disaccharide Analysis. Hexasaccharides (100 μg) were completely digested with a combination of heparinases I, II, and III (2 mU of each) and analyzed for disaccharide composition, by SAX-HPLC, as described previously.[10]

Mass Spectrometry. MS analysis was carried out on 0.24 μL of sample solution (20 ng) on a Bruker Esquire HCT ion trap mass spectrometer. Samples were injected into the source using a Cole Parmar syringe pump running at 4 μL/min. Full scan mass spectra (50–3000 Th) were acquired in negative ion electrospray mode using the Esquire Control software, and spectra were processed using Bruker's Data Analysis software.

NMR Spectroscopy. For NMR measurements, 2 mg of hexasaccharide was dissolved in 250 μL of 0.15 M NaCl, 20 mM $NaPO_4$, D_2O at pD 7.2 and then repeatedly exchanged in 1 mL of D_2O with intermediate lyophilization. For analysis, samples were contained in a 5 mm Shigemi tube at a sample volume of 250 μL. ^1H NMR spectra were acquired on a Bruker NMR spectrometer operating at a ^1H frequency of 500 MHz. Reported chemical shifts are in ppm relative to tetramethylsilane. The TOCSY and NOESY spectra were recorded in phase-sensitive mode using states-TPPI. A total of 256 experiments of 2048 data points were recorded with 128 scans over a spectral width of 2741 kHz in both dimensions. The FIDs were zero filled in F1 and multiplied by phase-shifted sine functions in both dimensions to give data sets of 1024 × 1024 points.

The DQF-COSYs were recorded in magnitude mode using the same size data set as above but with the number of scans reduced to 64. The FIDs were zero filled in F1 and multiplied by sine functions in both dimensions prior to transformation.

Molecular Modeling. Molecular modeling was carried out using the AMBER 8 molecular modeling suite.[29] Initial coordinates for the methyl glycosides of IdoUA and IdoUA(2S) in the $^1C_4$ conformation were based on geometries taken from the protein data bank file 1HPN.[30] These structures were then submitted to the antechamber module of AMBER 8, and AM1-BCC charges[31] and GAFF atom types were assigned.[32] The $^2S_0$ and $^4C_1$ geometries were taken from a 5 ns generalized Born implicit solvent molecular dynamic (MD) simulation of the $^1C_4$ models at a temperature of 400 K. At this temperature, a number of transitions occur between all three conformations (data not shown). AM1-BCC charges were then reassigned for randomly chosen $^2S_0$ and $^4C_1$ structures.

For explicit water simulations, each conformation was placed in a truncated octahedral box of explicit TIP3P water molecules. An 8 Å buffer of water was generated around the monosaccharide to the edge of the water box in each dimension. The charge on the monosaccharides was then neutralized through the addition of sodium ions using the addions method implemented in the xleap module.

Standard molecular modeling techniques were then used to equilibrate the system prior to a 1 ns 300 K molecular dynamics (MD) run. Briefly, during equilibration the initial positions of water molecules and sodium ion(s) were minimized while the conformation of the sugar was restrained (50 kcal mol^{-1} Å^{-1}). The restraints were then removed and the whole system minimized before weak restraints were reapplied to the sugar (10 kcal mol^{-1} Å^{-1}), and the system was allowed to heat to 300 K at constant volume for 20 ps. Restraints were again removed, and the density of the water was then allowed to relax during 100 ps of MD using a constant pressure periodic boundary with an average pressure of 1 atm. During this final equilibration step and the subsequent MD run, the temperature was maintained at 300 K. In all equilibration steps and MD runs, the Particle Mesh Ewald electrostatic treatment was implemented using the sander default settings and a cutoff distance of 6 Å. The SHAKE algorithm was also applied to all bonds involving hydrogen, and a 2 fs MD time step was used. The system coordinates were output to a trajectory file every picosecond, resulting in a final trajectory file for each MD run consisting of 1000 frames.

(28) Laemmli, U. K. *Nature* **1970**, *227*, 680–685.

(29) Case, D. A.; Darden, T. E.; Cheatham, T. E., III; Simmerling, C. L.; Wang, J.; Duke, R. E.; Luo, R.; Merz, K. M.; Wang, B.; Pearlman, D. A.; Crowley, M.; Brozell, S.; Tsui, V.; Gohlke, H.; Mongan, J.; Hornak, V.; Cui, G.; Beroza, P.; Schafmeister, C.; Caldwell, J. W.; Ross, W. S.; Kollman, P. A. University of California: San Francisco, CA, 2004.

(30) Mulloy, B.; Forster, M. J.; Jones, C.; Davies, D. B. *Biochem. J.* **1993**, *293*, 849–858.

(31) Jakallan, A.; Jack, D. B.; Bayly, C. I. *J. Comput. Chem.* **2002**, *23*, 1623–1641.

(32) Wang, J.; Wolf, R. M.; Caldwell, J. W.; Kollman, P. A.; Case, D. A. *J. Comput. Chem.* **2004**, *25*, 1157–1174.
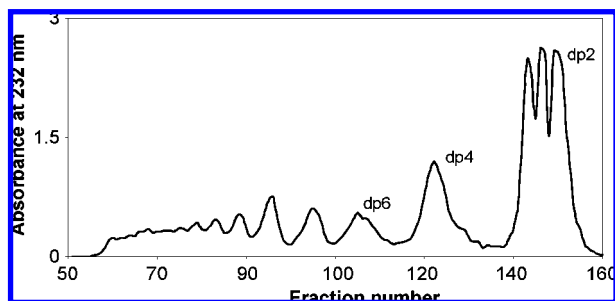
Figure 2. Bio-Gel filtration profile of HS after cleavage with heparinase III. HS after incubation with heparinase III was chromatographed on a Bio-Gel P10 gel filtration column (3 × 120 cm). Fractions were monitored for absorbance at 232 nm.

The program mdXvu was used to analyze the explicit water MD trajectories and extract theoretical coupling constants for the sugar in each frame according to the Haasnoot et al. equation.[33] It was also used to monitor values of the Cremer−Pople ring puckering parameters θ and θ_2 (pyranose ring atoms were selected in the order O5−C1−C2−C3−C4−C5).

Constrained Least-Squares Analysis. The sum of the squares of the differences between each of the experimentally observed coupling constants and a weighted average of the theoretical coupling constants was minimized. For iduronates, the weighted average of the theoretical constants was represented by the formula:

$$aJ_{x,y}{}^1C_4 + bJ_{x,y}{}^4C_1 + cJ_{x,y}{}^2S_0 \tag{1}$$

where $J_{x,y}$ is the theoretical value for each coupling constant $J_{1,2}$, $J_{2,3}$, $J_{3,4}$, and $J_{4,5}$, and for ΔUA by

$$aJ_{x,y}{}^1H_2 + bJ_{x,y}{}^2H_1 \tag{2}$$

where $J_{x,y}$ is the theoretical value for each coupling constant $J_{1,2}$, $J_{2,3}$, and $J_{3,4}$.

The sum of the squares of the differences was minimized by varying parameters a, b, and c subject to the constraints that their sum should equal 1 and each could take a value ≥ 0 but ≤ 1. The percentages of each conformation reported are parameters a, b, or c expressed as a percentage of their sum total 1.

Results

Isolation and Assessment of Hexasaccharide Purity. HS was exhaustively digested using heparinase III and fractionated on Bio-Gel P10 (Figure 2). This afforded fractions of size-uniform oligosaccharides. The hexasaccharide fraction was then further purified by charge fractionation using semipreparative SAX-HPLC (Figure 3). The presence of multiple similarly charged hexasaccharides under six groups of peaks labeled 6-1 to 6-6 was assessed using PAGE (inset in Figure 3). Based on these results, 6-2 and 6-3 were deemed to contain a single hexasaccharide structure, respectively, and were taken on for further analysis.

Disaccharide and Mass Spectrometry Analysis. The disaccharide compositions of 6-2 and 6-3 were determined (Table 1). This indicated that both oligosaccharides carried three sulfate groups. This was confirmed by mass spectrometry. The theoretical mass of a fully protonated oligosaccharide composed of a 1:1:1 ratio of the three disaccharides as indicated by the disaccharide analysis is 1294.04 Da (M). Both samples produced almost identical spectra (data not shown) with the major ions observed corresponding to $[M - 3H]^{-3}$ and $[M - 3H + Na]^{-2}$.
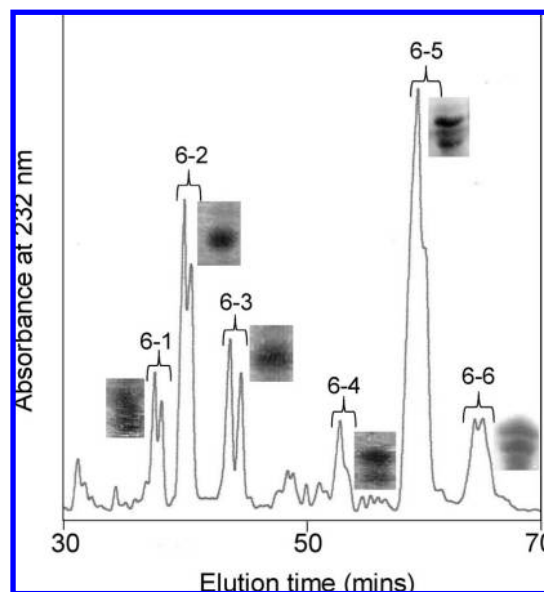
(33) Haasnoot, C. A. G.; de Leeuw, F. A. A. M.; Altona, C. *Tetrahedron* **1979**, *36*, 2783−2792.

Figure 3. Semipreparative SAX chromatography of the heparinase III resistant hexasaccharides. The hexasaccharide fraction was applied to a ProPac PA-1 SAX-HPLC column (9 × 250 mm) and eluted with a linear gradient of 0−1 M NaCl in distilled water, pH 3.5, over 80 min at a flow rate of 4 mL/min. The eluate was monitored for absorbance at 232 nm, and 2 mL fractions were collected. Insets show the PAGE analysis for each fraction pooled 6-1−6-6 (see Materials and Methods).

NMR Analysis. The one-dimensional ^{1}H NMR spectra of hexasaccharides 6-2 and 6-3 were recorded (Figure 4). Two-dimensional COSY, TOCSY (120 ms mixing time), NOSEY (500 ms mixing time), and HSQC (not shown) NMR spectra were also recorded for both oligosaccharides (Figure 5). The chemical shifts around 2 ppm, which correspond to the methyl protons of the *N*-acetyl groups, are not shown in any of the 2D NMR figures, and no through-bond cross-peaks were detected in the COSY and TOCSY spectra for all three protons. Also, no through-space connectivities were detected for these protons in any recorded NOESY spectra. The resonance immediately downfield from the H4 terminal UA proton does not couple to any oligosaccharide proton(s) in any of the 2D spectra.

Chemical shifts were assigned using 2D COSY, TOCSY, and NOESY analysis as described below. *trans*-Glycosidic NOEs between the anomeric proton H-1 and H-4 of the following monosaccharide allowed the relative positioning of each monosaccharide within the oligosaccharide chain to be established. On complete assignment of the proton chemical shifts, a HSQC spectrum was acquired (data not shown). Assignment of the ^{13}C chemical shifts was based on the observation of ^{1}H−^{13}C signal correlation in the HSQC spectrum. The ^{1}H and ^{13}C assignments are summarized in Table 2.

Ring protons of the terminal UA (residue a) of hexasaccharide 6-2 were assigned directly from the COSY spectra (Figure 5A). A single *trans*-glycosidic cross-peak was identified in the NOESY spectrum (Figure 5C) from H1 of UA to an unassigned proton of the linking glucosamine (residue b) at 3.866 ppm. The TOCSY spectrum (Figure 5B) was used to assign the anomeric proton H1 (5.336 ppm) of the ring system containing the 3.866 ppm unassigned glucosamine proton. The COSY spectrum was then used to assign the ring protons H2, H3, and H4 (3.866 ppm). Proton H5 and both H6 protons were assigned by a combined HSQC (spectrum not shown), TOCSY, and COSY analysis. Assignment of H2 to 3.314 ppm identified this glucosamine as being *N*-sulfated. Two *trans*-glycosidic cross-

Table 1. Disaccharide Composition and Mass Spectrometry Analysis of Hexasaccharides 6-2 and 6-3[a]

hexasaccharide	ΔUA-GlcNAc	ΔUA-GlcNS	ΔUA(2S)-GlcNS	major ions observed
6-2	1.08	1.00	0.85	430.34 $[M - 3H]^{-3}$
				656.84 $[M - 3H + Na]^{-2}$
6-3	1.03	1.00	1.03	430.13 $[M - 3H]^{-3}$
				656.52 $[M - 3H + Na]^{-2}$

[a] Hexasaccharides 6-2 and 6-3 were digested to disaccharides with a combination of heparinases I−III and analyzed by SAX-HPLC. Data are shown as molar ratios relative to the common disaccharide ΔUA-GlcNS. The major ions of the intact hexasaccharides detected by mass spectrometry are as shown.
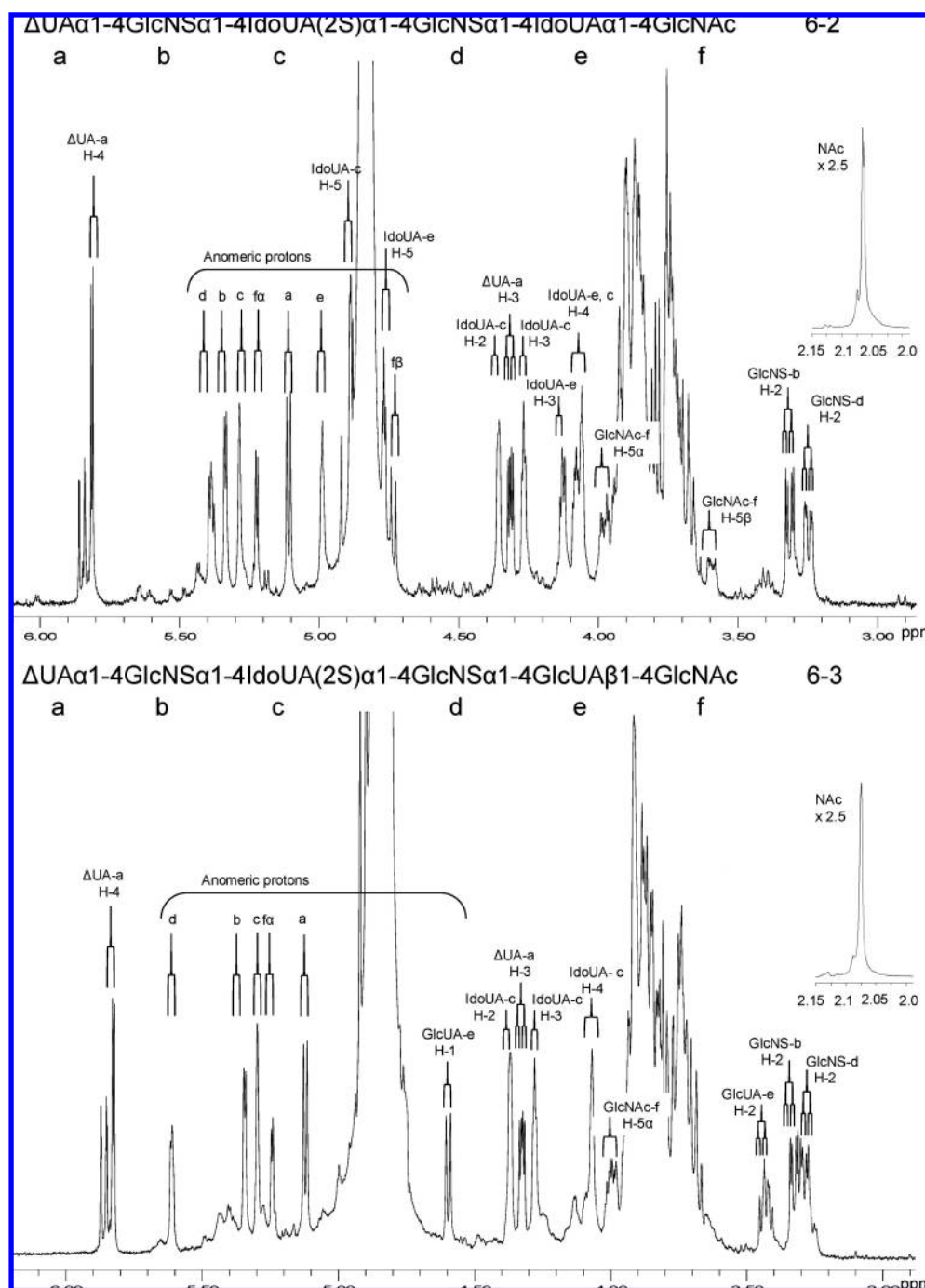

Figure 4. One-dimensional 500 MHz ^{1}H NMR spectra of hexasaccharides 6-2 and 6-3. Spectra were recorded in 0.15 M NaCl, 20 mM NaPO$_4$, D$_2$O at pD 7.2 and 25 °C.

peaks were identified in the NOESY spectrum to unassigned protons in the adjacent IdoUA (residue c) at 4.059 and 4.266 ppm. Once again, the TOCSY spectrum was used to assign the anomeric H1 proton (5.285 ppm) for the ring system containing these unassigned IdoUA protons. Protons H2, H3 (4.266 ppm), H4 (4.059 ppm), and H5 were identified from the COSY
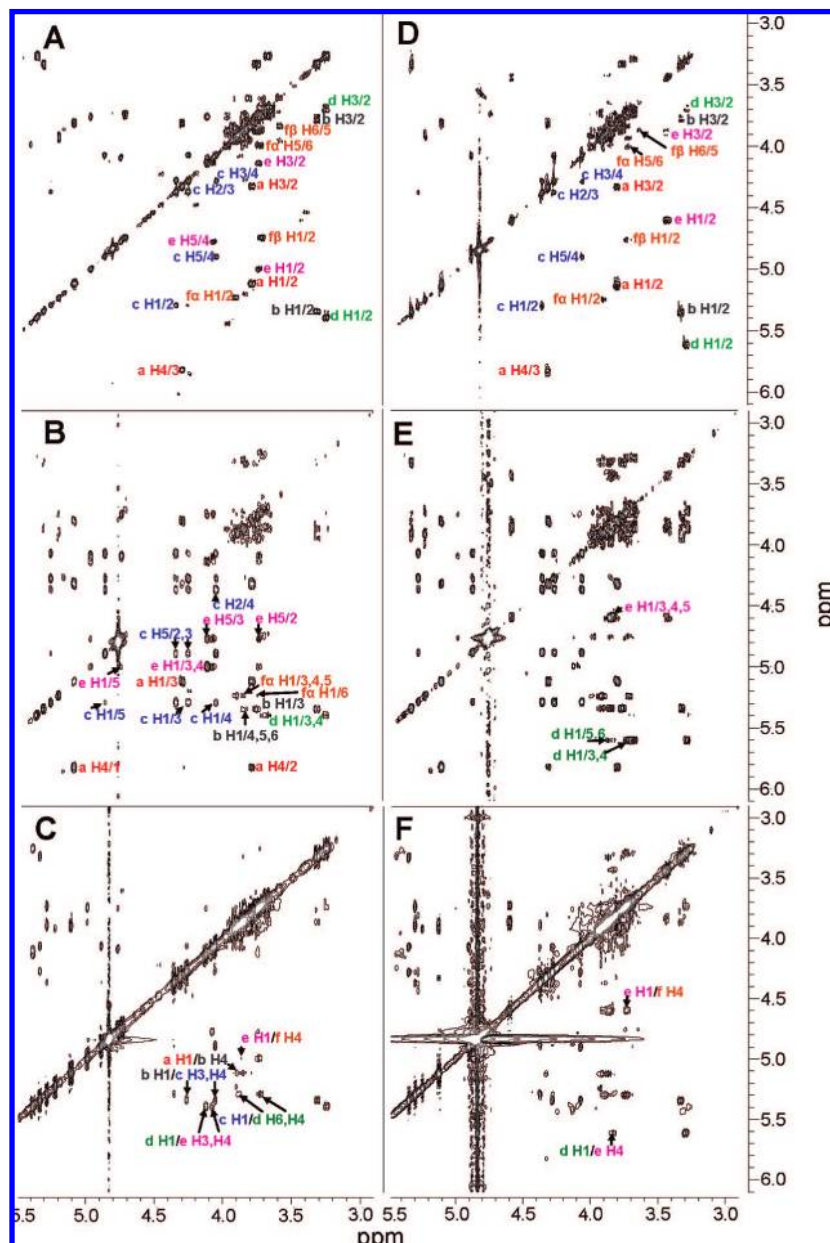
Figure 5. Two-dimensional 500 MHz ¹H NMR spectra of hexasaccharides 6-2 and 6-3. COSY (6-2 panel A, 6-3 panel D), TOCSY (6-2 panel B, 6-3 panel E), and NOESY (6-2 panel C, 6-3 panel F). The first proton given in each peak label is assigned in the F1 dimension (vertical scale).

spectrum, identifying H3 and H4, as the protons involved in the *trans*-glycosidic NOEs from H1 of residue b. Assignment of H2 to 4.356 ppm identified this IdoUA residue as being 2-*O*-sulfated. Two *trans*-glycosidic cross-peaks were observed in the NOESY spectrum between H1 of the IdoUA(2S) (residue c) and two unassigned protons in the next glucosamine (residue d) at 3.72 and 3.889 ppm. The anomeric proton H1 for the ring system containing these unassigned protons was assigned to 5.391 ppm, using the TOCSY spectrum. The COSY spectrum allowed assignment of H2, H3, and H4 (3.72 ppm), hence identifying H4 as one of the two protons involved in the *trans*-glycosidic NOE between residues c and d. Proton H5 and both H6 protons (range 3.889−3.905 ppm) were assigned by combined HSQC, TOCSY, and COSY analysis; this allowed the identification of one of the H6 protons as being the missing *trans*-glycosidic NOE contact with H1 of residue c. Assignment of H2 to 3.247 ppm identified this glucosamine as being *N*-sulfated. Two *trans*-glycosidic cross-peaks were identified in

the NOESY spectrum from H1 of GlcNS (residue d) to unassigned protons of the next IdoUA (residue e) at 4.079 and 4.128 ppm. The anomeric proton H1 (4.989 ppm) for the ring system containing the two unassigned IdoUA protons was identified from the TOCSY spectrum. Protons H2, H3 (4.128 ppm), H4 (4.079 ppm), and H5 were assigned from the COSY spectrum, and this identified protons H3 and H4, as the protons involved in the *trans*-glycosidic NOEs from H1 of residue d. Assignment of H2 to 3.743 ppm identified this IdoUA as being unsulfated at position 2. A single *trans*-glycosidic cross-peak was identified in the NOESY spectrum from H1 of IdoUA (residue e) to an unassigned proton in the reducing terminal glucosamine (residue f) at 3.86 ppm. The TOCSY spectrum identified two ring systems containing the 3.86 ppm unassigned glucosamine proton, representing the α and β anomeric configurations of the reducing terminal GlcNAc residue. The anomeric protons for each configuration were assigned to α (5.224 ppm) and β (4.734 ppm), and protons H2 and H3 (3.837

Table 2. ^{1}H and ^{13}C Chemical Shift Assignments for Hexasaccharides 6-2 and 6-3^a

	residue			6-2			6-3	
a	ΔUA	H1	5.11 (6.9)	C1	100.947	H1	5.122 (6.6)	C1	101.108
		H2	3.801 (6.3)	C2	70.694	H2	3.813 (6.0)	C2	70.693
		H3	4.314 (3.1)	C3	67.296	H3	4.325 (3.4)	C3	67.296
		H4	5.814	C4	107.903	H4	5.825	C4	107.741
				C5	n.d.			C5	n.d.
				C6	n.d.			C6	n.d.
b	GlcNSO$_3$	H1	5.336 (3.4)	C1	97.226	H1	5.343 (3.5)	C1	97.063
		H2	3.314 (10.7)	C2	57.913	H2	3.327 (10.7)	C2	57.913
		H3	3.761	C3	n.d.	H3	3.77	C3	n.d.
		H4	3.866	C4	n.d.	H4	3.885	C4	n.d.
		H5	3.837	C5	n.d.	H5	3.85	C5	n.d.
		H6	3.837−3.925	C6	n.d.	H6	3.797−3.966	C6	n.d.
		H6′	3.837−3.925			H6′	3.797−3.966		
c	IdoUA(2S)	H1	5.285 (1.6)	C1	99.167	H1	5.297 (1.6)	C1	99.167
		H2	4.356 (4.1)	C2	74.415	H2	4.368 (4.1)	C2	74.576
		H3	4.266 (3.15)	C3	67.62	H3	4.279 (3.15)	C3	67.458
		H4	4.059 (2.2)	C4	75.547	H4	4.068 (1.5)	C4	75.547
		H5	4.885	C5	68.105	H5	4.896	C5	68.267
				C6	n.d.			C6	n.d.
d	GlcNSO$_3$	H1	5.391 (3.4)	C1	95.446	H1	5.613 (3.7)	C1	97.549
		H2	3.247 (10.1)	C2	58.075	H2	3.288 (10.1)	C2	58.236
		H3	3.743	C3	n.d.	H3	3.683	C3	n.d.
		H4	3.72	C4	n.d.	H4	3.741	C4	n.d.
		H5	3.854	C5	n.d.	H5	3.823	C5	n.d.
		H6	3.889−3.905	C6	n.d.	H6	3.891−3.966	C6	n.d.
		H6′	3.889−3.905			H6′	3.891−3.966		
e	IdoUA (6-2)	H1	4.989 (2.5)	C1	101.755	H1	4.596 (7.8)	C1	102.24
	GlcUA (6-3)	H2	3.743 (5.0)	C2	69.238	H2	3.428	C2	72.797
		H3	4.128 (3.3)	C3	68.429	H3	3.895	C3	n.d.
		H4	4.079 (2.8)	C4	74.9	H4	3.828	C4	n.d.
		H5	4.767	C5	69.238	H5	3.813	C5	n.d.
				C6	n.d.			C6	n.d.
f	GlcNAc (α)	H1	5.224 (3.4)	C1	90.593	H1	5.242 (3.1)	C1	90.431
		H2	3.905	C2	n.d.	H2	3.905	C2	n.d.
		H3	3.837	C3	n.d.	H3	3.934	C3	n.d.
		H4	3.86	C4	n.d.	H4	3.726	C4	n.d.
		H5	3.979	C5	n.d.	H5	3.996	C5	n.d.
		H6	3.725−3.754	C6	n.d.	H6	3.842−3.89	C6	n.d.
		H6′	3.725−3.754			H6′	3.842−3.89		
		NAc	2.064	NAc	21.998	NAc	2.075	NAc	21.998
	GlcNAc (β)	H1	4.734 (8.1)	C1	94.961	H1	4.757	C1	94.799
		H2	3.725	C2	n.d.	H2	3.735	C2	n.d.
		H3	3.86	C3	n.d.	H3	3.726	C3	n.d.
		H4	3.931	C4	n.d.	H4	4.00	C4	n.d.
		H5	3.591	C5	n.d.	H5	3.644	C5	n.d.
		H6	3.808−3.837	C6	n.d.	H6	3.847−3.89	C6	n.d.
		H6′	3.808−3.837			H6′	3.847−3.89		
		NAc	2.064	NAc	21.998	NAc	2.075	NAc	21.998

^{a} Coupling constants (in Hz) to the next proton listed are given in parentheses. n.d.: not determined because of overlapping signals.

ppm, α and 3.86 ppm, β) were assigned for both anomers using the COSY spectrum. Assignment of H2 to 3.905 ppm (α) and 3.725 ppm (β) confirmed the glucosamine to be *N*-acetylated. Protons H4 (3.86 ppm, α and 3.931 ppm, β), H5, and the H6's were assigned by a combined HSQC, TOCSY, and COSY analysis. This identified protons H3 (β) and H4 (α) as potentially being involved in the glycosidic NOE with H1 of residue e. A detailed proton assignment of 6-3 was also carried out, and this established the first three residues to be identical in nature and sequence to those of 6-2. The notable variation between the two oligosaccharides occurred in the chemical shift values of protons H1 and H2 of the adjoining GlcNS (residue d) and in the nature of the GlcUA (residue e). Two *trans*-glycosidic cross-peaks were identified in the NOESY spectrum (Figure 5F), from H1 of IdoUA(2S) (residue c) to two unassigned protons in the adjacent glucosamine (residue d) at 3.741 and 3.891 ppm. The anomeric proton H1 was assigned to 5.613 ppm from the TOCSY spectrum. Protons H2, H3, and H4 (3.741 ppm) were assigned from the COSY spectrum (Figure 5D), identifying H4

as one of the two protons involved in the *trans*-glycosidic NOEs from residue c. Protons H5 and the H6's (range 3.891−3.966 ppm) were later assigned by a combined HSQC, TOCSY, and COSY analysis; this identified one of the H6 protons as forming the remaining *trans*-glycosidic NOE with residue c. Assignment of H2 to 3.288 ppm identified the glucosamine as being *N*-sulfated. A single *trans*-glycosidic cross-peak was identified in the NOESY spectrum from H1 of GlcNS (residue d) to an unassigned proton in the proceeding GlcUA (residue e) at 3.828 ppm. The TOCSY spectrum (Figure 5E) allowed assignment of the anomeric proton H1 of residue e to 4.596 ppm, identifying this residue as GlcUA and not IdoUA as in 6-2. Protons H2, H3, and H4 (3.828 ppm) were assigned by COSY analysis identifying H4 as the proton involved with the *trans*-glycosidic NOE from residue e. Proton H5 was assigned using a combined HSQC, TOCSY, and COSY analysis, and a single *trans*-glycosidic cross-peak was identified in the NOESY spectrum from H1 of GlcUA (residue e) to an unassigned proton in the reducing terminal glucosamine (residue f) at 3.726 ppm. The
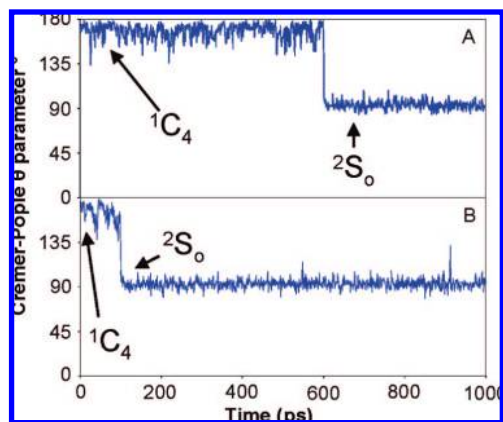
Figure 6. Values of the Cremer–Pople ring puckering parameter $\theta°$ for iduronates starting in the $^1C_4$ conformation over the course of a 1 ns 300 K MD simulation. $^1C_4$ geometries are characterized by values of θ of around 180° and $^4C_1$ by values of around 0°. $^2S_0$ conformations are characterized by a θ value between around 90° and by a second parameter Φ_2 around 150°. Both IdoUA(2S) $^1C_4$ (panel A) and IdoUA $^1C_4$ (panel B) made a conformational transition to the $^2S_0$ conformation during the course of the MD run. The average and standard errors of θ and Φ_2 parameters after transition were 93.4° ± 4.1 and 155° ± 14.23 (panel A) and 92.9° ± 4.5 and 152.2° ± 11.56 (panel B), confirming them to be the $^2S_0$ conformation. These averages are comparable to those seen when the MD simulation is started in the $^2S_0$ geometry (see main text).

Table 3. The Average Value of the Theoretical Coupling Constants, Obtained from Explicit Water Molecular Dynamic Simulations[a]

	$^1C_4$	$^2S_0$	$^4C_1$
$^3J_{1,2}$ IdoUA	1.71 ± 0.53	4.36 ± 1.5	7.34 ± 0.64
IdoUA(2S)	1.78 ± 0.53	3.99 ± 1.39	7.28 ± 0.69
$^3J_{2,3}$ IdoUA	1.56 ± 0.99	9.25 ± 1.04	9.05 ± 1.02
IdoUA(2S)	1.82 ± 0.94	9.26 ± 1.04	8.86 ± 1.1
$^3J_{3,4}$ IdoUA	2.01 ± 0.93	5.78 ± 2.1	9.06 ± 0.79
IdoUA(2S)	2.32 ± 0.99	6.36 ± 1.94	9.12 ± 0.77
$^3J_{4,5}$ IdoUA	1.23 ± 0.7	4.26 ± 1.89	5.41 ± 1.06
IdoUA(2S)	1.1 ± 0.71	4.73 ± 1.91	5.15 ± 1.09

[a] Theoretical coupling constants were extracted from each molecular dynamic frame according to the Haasnoot et al. equation. $^2S_0$ and $^4C_1$ coupling constants were averaged over 1000 MD trajectory frames. $^1C_4$ constants were averaged over 99 frames for IdoUA and 599 frames for IdoUA(2S).

TOCSY spectrum indicated two ring systems for the terminal residue f containing the unassigned proton at 3.726 ppm; again this was attributed to the presence of both α and β anomers of the terminal GlcNAc. The anomeric protons for each configuration were assigned to 5.242 ppm (α) and 4.757 ppm (β). Protons H2 and H3 (3.934 ppm, α and 3.726 ppm, β) were assigned for both anomers using the COSY spectrum. Assignment of H2 to 3.905 ppm (α) and 3.735 ppm (β) confirmed the glucosamine to be N-acetylated. Protons H4 (3.726 ppm, α and 4.000 ppm, β), H5, and the H6's were assigned by a combined HSQC, TOCSY, and COSY analysis. This implicated either one or both of protons H3 (β), peak centered on 3.726 ppm, and H4 (α), peak centered on 3.726 ppm, as being involved in the glycosidic NOE observed with residue e.

Molecular Modeling. Both IdoUA and IdoUA(2S) $^1C_4$ starting geometries made a transition to the $^2S_0$ conformation, at 99 ps for IdoUA and 599 ps for IdoUA(2S) (Figure 6). The average values and standard deviations for the coupling constants reported in Table 3 are taken over the duration of the $^1C_4$ conformation. No conformational transitions were observed for the $^2S_0$ and $^4C_1$ starting geometries (data not shown). The average Cremer–Pople ring puckering parameter θ for the $^4C_1$

conformation was 10.3 ± 5.6 for IdoUA(2S) and 9.0 ± 5.11 for IdoUA. The average for the $^2S_0$ conformation, over the whole 1 ns, was 93.1 ± 4.4 for IdoUA(2S) and 92.8 ± 4.5 for IdoUA. For the $^2S_0$ conformation, the additional average Φ_2 parameter, again over the whole 1 ns, was 159.8 ± 14.3 for IdoUA(2S) and 154.1 ± 16.0 for IdoUA. The average value and standard deviation for the coupling constants given in Table 3 for the $^2S_0$ and $^4C_1$ conformations were therefore taken over all 1000 frames of the MD trajectory.

Discussion

The hexasaccharides 6-2 and 6-3, characterized in this study, have previously been isolated from the cell surface of a cultured 3T3 fibroblast cell line.[27] Hexasaccharide 6-3 has also previously been isolated and sequenced from an alternate source of porcine HS.[26]

Initially, HPLC separation indicated that 6-2 and 6-3 may contain a number of oligosaccharides. The significant presence of more than one saccharide was however ruled out by the PAGE analysis and confirmed by the NMR analysis, where all anomeric chemical shifts could be assigned to a single oligosaccharide chain. The splitting observed with the 6-2 and 6-3 HPLC peaks is most probably due to the presence of both α and β anomeric configurations of the reducing end GlcNAc residue, with one configuration resulting in a slightly increased binding affinity to the stationary phase.

Least-square fitting was used to calculate the ΔUA and iduronate conformer populations best fitting our experimental NMR data. For the nonreducing terminal ΔUA of 6-2 and 6-3, the population distributions differed by only 2% when the theoretical coupling constants of Raggazzi et al.[21] or Bazin et al. (structure 22)[34] were used in our fitting procedure. Hence, the conformer population distributions of ΔUA are in excellent agreement with previous studies. For an oligosaccharide terminating in the sequence ΔUA-GlcNAc, it has been shown that the predominant conformation of ΔUA is $^2H_1$ (68.8%).[21] In comparison, our data (Table 4) show that replacement of the N-acetyl group by an N-sulfo group, for a terminal ΔUA-GlcNAc structure, has little effect on the conformational equilibrium of ΔUA.

For IdoUA and IdoUA(2S), significant differences in the calculated populations were found, depending on which of the published theoretical coupling constants were used.[35–40] The most illustrative example was iduronate position "a" (Table 4, indicated by an arrow) previously analyzed by Lucas et al.[38] Using our fitting procedure, and the original theoretical constants published by Lucas et al., the populational equilibrium is 79%: 21%:0% $^1C_4$:$^4C_1$:$^2S_0$. However, using an earlier set of theoretical coupling constants published by Ojeda et al.,[39] the populational equilibrium is 80%:0%:20% $^1C_4$:$^4C_1$:$^2S_0$. To prevent the choice

(34) Bazin, H. G.; Capila, I.; Linhardt, R. J. *Carbohydr. Res.* **1998**, *309*, 135–144.

(35) Ferro, D. R.; Provasoli, A.; Ragazzi, M.; Torri, G.; Casu, B.; Gatti, G.; Jacquinet, J. C.; Sinay, P.; Petitou, M.; Choay, J. *J. Am. Chem. Soc.* **1986**, *108*, 6773–6778.

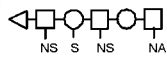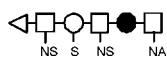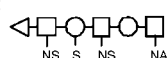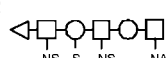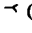(36) Forster, M. J.; Mulloy, B. *Biopolymers* **1993**, *33*, 575–588.
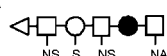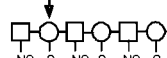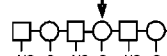
(37) Hricovini, M.; Scholtzova, E.; Bizik, F. *Carbohydr. Res.* **2007**, *342*, 1350–6.

(38) Lucas, R.; Angulo, J.; Nieto, P. M.; Martin-Lomas, M. *Org. Biomol. Chem.* **2003**, *1*, 2253–2266.

(39) Ojeda, R.; Angulo, J.; Nieto, P. M.; Martin-Lomas, M. *Can. J. Chem.* **2002**, *80*, 917–936.

(40) van Boeckel, C. A. A.; van Aelst, S. F.; Wagenaars, G. N.; Mellema, J. R.; Paulsen, H.; Peters, T.; Pollex, A.; Sinnwell, V. *Recl. Trav. Chim. Pays-Bas* **1987**, *106*, 19–29.

Table 4. Conformer Populations of the ΔUA and Iduronate Residues within Hexasaccharides 6-2 and 6-3[a]

	$^1H_2$	$^2H_1$		$J_{1,2}$	$J_{2,3}$	$J_{3,4}$	$J_{4,5}$	Sum of square differences
ΔUA	%	%		Hz	Hz	Hz		
6-2	25	75		6.9	6.3	3.1	-	0.11
6-3	31	69		6.6	6.0	3.4	-	0.03
	$^1C_4$	$^4C_1$	$^2S_0$					
Non-sulfated IdoUA	%	%	%					
6-2	57	0	43	2.5	5.0	3.3	2.8	0.32
Sulfated IdoUA								
6-2	73	0	27	1.6	4.1	3.15	2.2	0.75
6-3	76	0	24	1.6	4.1	3.15	1.5	0.99
Lucas et al.								
a	64	18	18	3.6	4.2	3.6	3.5	1.72
b	60	28	12	3.6	4.3	4.5	3.7	1.25

Symbols:

◁ ΔUA   ● GlcUA   ○ IdoUA   IdoUA(2S)   ☐ GlcNAc
                                                  S   NA

☐ GlcNS   ↜ O-isopropyl
NS

[a] For comparison, two oligosaccharides synthesized by Lucas et al. are also included in the table (see Discussion). The minimized sum of the square differences is shown as a guide to how well the calculated population ratios fit the experimental data.

of theoretical constants biasing the fitting procedure, 1 ns explicit water molecular dynamic simulations were carried out on the methyl glycoside of iduronates, in either the $^1C_4$, $^4C_1$, or $^2S_0$ starting conformations. The theoretical coupling constants used for fitting were then an average taken over the course of the MD run, as given in Table 3. While the dynamics and resulting coupling constants may be slightly altered, as iduronates 6-2 and 6-3 are incorporated into an oligosaccharide chain,[36] the use of averaged coupling constants obtained in this way eliminates the high level of bias achieved by choosing to fit to a single set of theoretical values. The use of explicit water molecules also counteracts the tendency for iduronate conformations to be adopted that are dominated by intramolecular hydrogen bonds. Such conformations could be expected to result from quantum mechanical calculations in which the molecule is treated in vacuo,[41] as recently carried out by Hricovini et al.[37] While it is not known to what extent the balance between intra- and intermolecular hydrogen bonding influences iduronate

conformational behavior, the neglect of hydrogen bonding between the sugar and solvent in theoretical iduronate coupling constant studies must surely be considered an important oversight. Additionally, improper dihedral angles imposed to prevent $^1C_4$ to $^2S_0$ transitions by Verli et al.[42] were not used, as it was thought these constraints may detrimentally influence the dynamics of the pyranose ring system to which they were applied. For comparative purposes, all experimentally measured coupling constants mentioned subsequently have been refitted using our MD-averaged coupling constants (Table 3).

The sulfation sequence GlcNS-IdoUA-GlcNS has been studied previously[40] and was refitted, using our coupling constants, to 52%:0%:48%, $^1C_4$:$^4C_1$:$^2S_0$. Our data (Table 4) indicate that replacement of the *N*-sulfo group to the right (reducing side) of the IdoUA in this sequence by an *N*-acetyl group has little impact on the balance of the IdoUA equilibrium.

The sulfation sequence GlcNS-IdoUA(2S)-GlcNS occurs twice within a hexasaccharide recently synthesized by Lucas

(41) Imberty, A.; Perez, S. *Chem. Rev.* **2000**, *100*, 4567–4588.

(42) Verli, H.; Guimaraes, J. *Carbohydr. Res.* **2004**, *339*, 281–290.

Table 5. Observed Interglycosidic NOEs for Hexasaccharides 6-2 and 6-3

glycosidic linkage	6-2	6-3
1−2	H1′−H4	H1′−H4
2−3	H1′−H4	H1′−H4
	H1′−H3	H1′−H3
3−4	H1′−H4	H1′−H4
	H1′−H6[a]	H1′−H6[a]
4−5	H1′−H4	H1′−H4
	H1′−H3	
5−6	H1′−H4	H1′−H4

[a] Either H6 *pro*R or H6 *pro*S, underdetermined due to overlapping NMR peaks.

et al.,[38] and experimental coupling constants were reported. This showed a distribution of 64%:18%:18%, $^1C_4$:$^4C_1$:$^2S_0$ for position a and 60%:28%:12%, $^1C_4$:$^4C_1$:$^2S_0$ for position b, when refitted to our theoretical coupling constant data. For the same sulfation sequence occurring in 6-2 and 6-3, no contribution from the $^4C_1$ conformation was seen (Table 4). It should be noted that no further experimental coupling constant data could be found in the literature for the GlcNS-IdoUA(2S)-GlcNS sequence.

The sulfation sequence GlcNS(6S)-IdoUA(2S)-GlcNS has been previously analyzed[40] and was refitted to 59%:0%:41% $^1C_4$:$^4C_1$:$^2S_0$. A comparison of the balance of this equilibrium to the balance of the IdoUA(2S) equilibrium in 6-2 and 6-3, with no flanking 6-*O*-sulfo group and predominantly $^1C_4$ (Table 4), suggests the addition of 6-*O*-sulfation alters the balance of the equilibrium more toward $^2S_0$. However, studies of the sequence GlcNAc(6S)-IdoUA(2S)-GlcNS[40] refitted to 83%:0%:17% $^1C_4$:$^4C_1$:$^2S_0$ suggest a cooperative effect for *N*- and 6-*O*-sulfation to the left (nonreducing side) of IdoUA(2S) with neither *N*- nor 6-*O* sulfation alone able to exert an influence toward $^2S_0$. Interestingly, the cooperative effect of *N*- and 6-*O*-sulfation is seen in analysis of the sequence GlcNS-IdoUA(2S)-GlcNAc(6S)[39] refitted to 50%:0%:50% $^1C_4$:$^4C_1$:$^2S_0$. This sequence suggests that *N*- and 6-*O* sulfation may not have to occur on the same glucosamine to influence the conformation more toward $^2S_0$ or that 6-*O*-sulfation/*N*-acetylation on the reducing flanking glucosamine may play a role in this. However, conformation of this must wait for an experimental measurement of iduronate coupling constants for the highly unusual GlcNAc-IdoUA(2S)-GlcNAc(6S), which has not yet been published. Within HS domains, 6-*O*-sulfation appears to be under tight regulatory control, and a number of in vivo studies have implicated this as an important regulatory feature in developmental processes.[43−46] The ability of 6-*O*-sulfation to influence the three-dimensional structure of HS could reflect its importance in regulating not only its own biosynthesis, but also its interaction with a range of proteins involved in critical biological processes.

The overall three-dimensional shape of both hexasaccharides can be determined from the observed inter-residue NOE patterns (Table 5). All of the *trans*-glycosidic NOEs observed are qualitatively similar to those observed in a number of synthetic and heparin-derived saccharides.[47] There is no reason to assume the secondary structure of 6-2 and 6-3 differs greatly from the overall helical conformation of these structures. However, their charge distributions must be subtly different from each other for elution to occur from the HPLC column at differing salt concentrations. The lack of an observed H1′−H3 NOE across the GlcNS-GlcUA glycosidic linkage of oligosaccharide 6-3 (Table 5) might be expected as GlcUA is in the $^4C_1$ conformation. This may place the associated carboxyl group in a more favorable position to interact with the charged groups of the HPLC column. Work is currently underway to investigate this through the development of an accurate charge model, consistent with the carbohydrate-specific Glycam molecular modeling force field.[48] Further molecular dynamic simulations may then reveal how such subtle conformational differences at the monosaccharide level alter the overall charge distribution of these and other HS oligosaccharides.

It is also interesting to speculate on the charge neutralization effects that would occur when charges on the sulfate groups, within HS chains, are neutralized by cationic groups on their binding proteins and the subsequent influence on IdoUA conformational transformations. At physiological salt concentrations, the charge on the sulfate groups could be expected to be neutralized by sodium counterions, when in free solution, and our MS spectroscopy data for both hexasaccharides show this to be the case. Additional charge neutralization, or exchange of sodium counterions for a protein cationic group, could influence the overall molecular shape of the heparan oligosaccharides via changes in IdoUA conformation. However, preferential binding may well occur to monosaccharide sequences in which iduronates are already predisposed to occur in the final conformation they will adopt upon protein binding, with this predisposition being dependent on the influence of sulfates and counterions flanking the flexible iduronates. Indeed, a change in counterions to Cu(II) has recently been shown to modify the activities of the FGF/FGFR signaling complex.[49]

There have been many conflicting reports concerning the structure/activity relationships of HS oligosaccharides. This has led to the suggestion that the interaction of HS oligosaccharides with other macromolecules is not strictly sequence specific.[50,51] The solution to this may be found in the conformational dynamics within HS chains, which centers on the conformational flexibility of the internal iduronates. The novel findings of this study will greatly enhance our knowledge of the influence of sequence/sulfation pattern on iduronate conformation and biological recognition, which could be key to our understanding of the mechanisms of HS-mediated signaling.

Note Added after ASAP Publication. Production errors were corrected in the last sentence of the Introduction and in reference citations in the third and fourth paragraphs of the Discussion. The corrected version was published September 10, 2008.

JA802863P

(43) Bullock, S. L.; Fletcher, J. M.; Beddington, R. S.; Wilson, V. A. *Genes Dev.* **1998**, *12*, 1894–906.

(44) Chen, E.; Stringer, S. E.; Rusch, M. A.; Selleck, S. B.; Ekker, S. C. *Dev. Biol.* **2005**, *284*, 364–76.

(45) Kamimura, K.; Fujise, M.; Villa, F.; Izumi, S.; Habuchi, H.; Kimata, K.; Nakato, H. *J. Biol. Chem.* **2001**, *276*, 17014–21.

(46) Lundin, L.; Larsson, H.; Kreuger, J.; Kanda, S.; Lindahl, U.; Salmivirta, M.; Claesson-Welsh, L. *J. Biol. Chem.* **2000**, *275*, 24653–60.

(47) Yamada, S.; Sakamoto, K.; Tsuda, H.; Yoshida, K.; Sugiura, M.; Sugahara, K. *Biochemistry* **1999**, *38*, 838–847.

(48) Woods, R. J.; Dwek, R. A.; Edge, C. J.; Fraser-Reid, B. *J. Phys. Chem.* **1995**, *99*, 3832–3846.

(49) Rudd, T. R.; Guimond, S. E.; Skidmore, M. A.; Duchesne, L.; Guerrini, M.; Torri, G.; Cosentino, C.; Brown, A.; Clarke, D. T.; Turnbull, J. E.; Fernig, D. G.; Yates, E. A. *Glycobiology* **2007**, *17*, 983–93.

(50) Kreuger, J.; Spillmann, D.; Li, J. P.; Lindahl, U. *J. Cell Biol.* **2006**, *174*, 323–7.

(51) Lindahl, U. *Thromb. Haemostasis* **2007**, *98*, 109–15.